IJNAOE
©SNAK, 2015

Int. J. Nav. Archit. Ocean Eng. (2015) 7:795~804
http://dx.doi.org/10.1515/ijnaoe-2015-0056
pISSN: 2092-6782, eISSN: 2092-6790

Numerical investigation of tip clearance effects on the performance of ducted propeller

Ding Yongle, Song Baowei and Wang Peng

School of Marine Science and Technology, Northwestern Polytechnical University, Xi'an, China

Received 3 Febuary2015; Revised 7 April 2015; Accepted 22 April 2015

ABSTRACT: *Tip clearance loss is a limitation of the improvement of turbomachine performance. Previous studies show the Tip clearance loss is generated by the leakage flow through the tip clearance, and is roughly linearly proportional to the gap size. This study investigates the tip clearance effects on the performance of ducted propeller. The investigation was carried out by solving the Navier-Stokes equations with the commercial Computational Fluid Dynamic (CFD) code CFX14.5. These simulations were carried out to determine the underlying mechanisms of the tip clearance effects. The calculations were performed at three different chosen advance ratios. Simulation results showed that the tip loss slope was not linearly at high advance due to the reversed pressure at the leading edge. Three type of vortical structures were observed in the tip clearance at different clearance size.*

KEY WORDS: Tip clearance; Ducted propeller; Computational fluid dynamic (CFD).

INTRODUCTION

Ducted propeller has been widely used in vessels and Autonomous Underwater Vehicles (AUVs) for decades. The duct propeller consists of an annular wing duct and a propeller. There are mainly two kinds of duct: the accelerating and the decelerating duct based on different kind of wing section. Since the accelerating duct is the most widely used, we only discuss this kind of duct in this paper.

A lot of experimental and theoretical researches have been done on ducted propellers (Kerwin et al., 1987; Abdel-Maksoud and Heinke, 2002; Hoekstra, 2006; Hsiao and Pauley, 1999; Hughes et al., 1992). One of the primary challenges for ducted propeller is the accurate prediction of hydrodynamic characteristics. The main limitations for the experimental and numerical prediction are the complex geometry and other technical problems (Park et al., 2005; Morgut and Nobile, 2012; Berchiche and Janson, 2008; Peng et al., 2013). An important factor influencing the accurate prediction of ducted propeller performance is the tip clearance or tip gap. The blade tip clearance between a blade and the duct has been the major source of many unfavourable flow phenomena. Complicated vortical structures are generated by the mixing of the two flows: the flow from the pressure side to the suction side through the clearance and the main flow and the injection of the flow into the boundary layers on the blade tip and the duct (You et al., 2007). These vortices often lead to noise, vibration, erosion and thrust/torque loss.

Corresponding author: *Wang Peng*, e-mail: *jerryd2014@163.com*

Quantitative studies on tip clearance of turbomachinery have been presented (Xiao et al., 2001; Mccarter et al., 2001; Booth, 1985; Yaras and Sjolander, 1992; Yaras et al., 1992). Most of these issues are focused on tip clearance flow in turbines, compressors and pumps. A basic understanding of the effect of the tip clearance is that the tip clearance generates complicated vortical structures which can result in performance decrease and rotating instabilities. In previous researches, the tip clearance loss grows roughly linearly with tip gap height. An proper approach to describe the tip clearance loss is the tip loss slope, i.e. the change in performance loss for a given change of Gap to Span Ratio (GSR) (Chima, 1998; Moon et al., 2002). Some researches have been developed emphasis on loss mechanisms of tip clearance. A series works on tip clearance loss have been done by Donghyun You and Meng Wang using large-eddy simulation (You et al., 2002; 2003; 2004; 2006).

Different with turbine and compressor, ducted propeller works in incompressible flow. Consequently, the heat transfer is neglected in numerical prediction. Ducted propeller works at a low advance ratio or high advance ratio occasionally. At high-advance ratios, ducted propeller generates complicated vortical structure which have effect on the blade tip loading. In turn, the blade tip pressure distribution could reverse at off-design points, which can change the vortical structure at the blade tip.

This paper aims to investigate the influence of tip clearance on the performance of ducted propeller. Considering the working condition of ducted propeller, the tip clearance effects are presented and compared at three different chosen advance ratios. These simulations are carried by solving the incompressible Navier-Stokes equations with a Multiple Reference Frame (MRF) method.

DUCTED PROPELLER MODEL

In this paper, calculations were carried out with a worldwide employed ducted propeller (the Ka4-70 propeller in 19A duct), which was presented by MARIN (Maritime Research Institute Netherland) (Oosterveld, 1970). The ducted propeller had a diameter of $D = 240$ *mm* and a pitch-diameter ratio of $P/D = 1$. The 19A duct was modified with a round trailing edge. The tip clearance of the propeller was set to 1 *mm* (about 0.42 percent of the propeller diameter D), which was the uniform clearance in the experiment research. Several difference models with tip clearance from 0 to 3 *mm* were used to investigate the effect on the performance of the ducted propeller.

NUMERICAL METHOD

The numerical simulations presented in this paper were carried out with the Ansys CFX14.5 (Ansys, 2012). The RANS solver with an Multiple Reference Frame (MRF) approach was used to predict the performance of the ducted propeller. The hydrodynamic equations were solved with the node-centered finite volume method. Considering that the propeller working in uniform flow, numerical predictions were carried out with single passage with rotational periodicity interface. Cavitation was not considered in all the simulations. All simulations were carried out in the water at 25℃ with a density of 997.0 kg/m^3 and a dynamic viscosity coefficient of 0.893×10^{-3} $kg/(m\cdot s)$. The advance speed is set to $V_A = 4$ *m/s*. The Reynolds number was computed based on the chord length at 0.75 span and the water speed with a result of 5.3×10^5.

Domains and meshes

The overall computational domain involves two parts as show in Fig. 1, the stationary domain (a cylinder) and the rotating domain which are part of a cylinder. The stationary domain should be large enough to avoid that the far field boundary conditions affect the prediction of the flow near the propeller. The rotating domain is a single passage containing one blade. The dimensions of both domains are given in Table 1.

Once the computational domains have been defined, boundary-fitted grid is required for the flow solver. As Morgut and Nobile (2012) performed, both the hex-structured meshes and the hybrid-unstructured meshes could guarantee with similar levels of accuracy. Nevertheless, the hex-structured meshes showed better performances for a detailed investigation of the local flow field. In this paper, the stationary domain was discretized with hex-structured meshes. For less grid generation efforts, hybrid-unstructured meshes had been employed on the rotating domain. Hex-structured meshes were used in predicting the details flow near the propeller and the duct. To present the detail of the flow near wall, boundary layers elements were employed

on the blade and the duct. The first element height of boundary layers was 0.05 *mm*, with a maximum Y-plus of 5.58, which is appropriate for the wall function for the flow inside the duct. Moreover, grids near the blade tip and in the clearance were refined with a finer mesh region, as showed in Fig. 2.

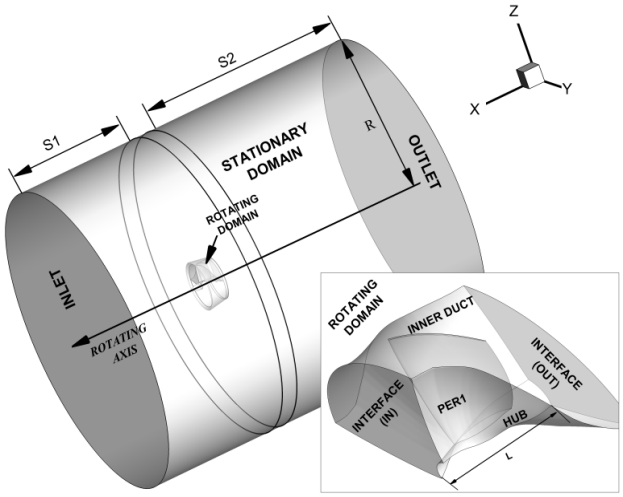

Fig. 1 Computational domain.

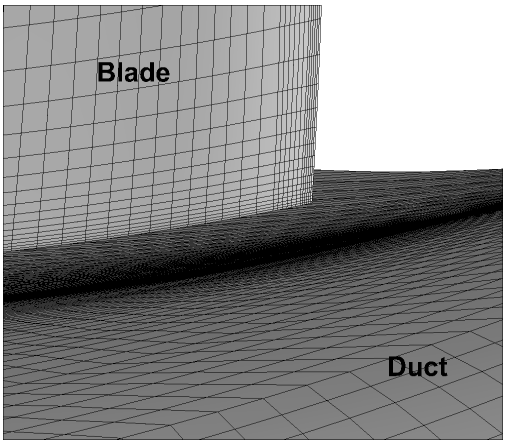

Fig. 2 Finer mesh region near blade tip and the tip clearance.

Table 1 Dimensions of the domains.

Locations	Size
S1	4D
S2	5D
R	3D
L	0.4D

The boundary conditions were defined as follows. On the inlet boundary a velocity inlet with turbulence intensity of 1% were set. On the outlet boundary a static pressure outlet with a reference pressure of 0 *Pa* was defined. On the periodic boundary the rotational periodicity was applied. On all solid surfaces the no slip boundary condition was defined. The free slip wall was applied on the cylinder face. Two sliding interfaces (the front face and the back face on the streamwise of the rotating domain) were defined between the stationary and the rotating domain, through which the flow properties are transmitted.

Verification and validation

For evaluating the effect of the clearance, the non-dimensional thrust and torque coefficients are given: the duct thrust coefficient K_{TN}, and the torque coefficient K_Q:

$$K_{TN} = \frac{T_N}{\rho n^2 D^4} \qquad K_T = \frac{T}{\rho n^2 D^4} \qquad K_Q = \frac{Q}{\rho n^2 D^5} \tag{1}$$

The ducted propeller efficiency is defined as:

$$\eta = \frac{J}{2\pi}\frac{K_T}{K_Q} \tag{2}$$

T_N is the duct thrust, $J = V_A / (nD)$ is the advance ratio and ρ, n and D represent the density of water, the Rotation Speed (RPS) and the propeller diameter respectively. The total thrust of the ducted propeller is $T = T_N + T_B$, where T_B is the blade thrust. The clearance size is represented as Gap to Span Ratio (GSR) which is defined as:

$$\text{GSR}=\frac{\text{Clearance size}}{\text{D}}\times 100 \tag{3}$$

The verification investigation of mesh dependency was carried out by evaluating the thrust coefficients with different mesh densities. Three levels of meshes having the same node distribution with difference node numbers were chosen for the simulations. As Table 2 shows, it indicates that the medium and the fine mesh have the same results substantially compared with the coarse mesh. Considering the computational efficiency and the accuracy, the medium level mesh was chosen for the simulations finally.

Table 2 Results of mesh dependency (J = 0.6, GSR = 0.5, VA = 4 *m/s*).

Mesh	Node number		K_T
	Stationary domain	Rotating domain	
Coarse	1465120	546536	0.18589
Medium	1465120	1491752	0.18857
Fine	1465120	1896048	0.18892

As Peng et al. (2013) suggested, eddy viscosity turbulence models are slightly better than Reynolds stress models in the prediction of tip vortex flow and the thrust and torque coefficients. Therefore, Standard $k-\varepsilon$, Realizable $k-\varepsilon$ and two-equation Shear-Stress Transport (SST) $k-\omega$ turbulence models were evaluated to verify the effect of turbulence model on the simulations. The relative percentage errors ΔK_t and ΔK_q were defined as Morgut and Nobile (2012) presented. As can be seen in Table 3, the results predicted by three turbulence models are at a similar level of accuracy. Two-equation SST $k-\omega$ turbulence was chosen for the simulations for the minimum ΔK_t.

$$\Delta K_t(\%) = \frac{K_{tCFD} - K_{tEXP}}{K_{tEXP}} \bullet 100 \qquad \Delta K_q(\%) = \frac{K_{qCFD} - K_{qEXP}}{K_{qEXP}} \bullet 100 \tag{4}$$

Table 3 Influence of turbulence models (J = 0.6, GSR = 0.5, VA = 4 *m/s*).

Model	ΔK_t	ΔK_q
Standard $k-\varepsilon$	-3.4	-2.2
Realizable $k-\varepsilon$	2.6	-3.5
Two-equation SST $k-\omega$	2.1	2.0

The results of simulations which are represented by the thrust coefficient, the torque coefficient and the propeller efficiency are compared with the experiment data. The maximum relative errors of thrust coefficient and the torque coefficient are 4.45% and 3.17% appear at $J = 0.7$ and $J = 0.4$ respectively. As presented in Fig. 3, the computed results of propeller open-water characteristics have a good agreement with the experimental data (Oosterveld, 1970).

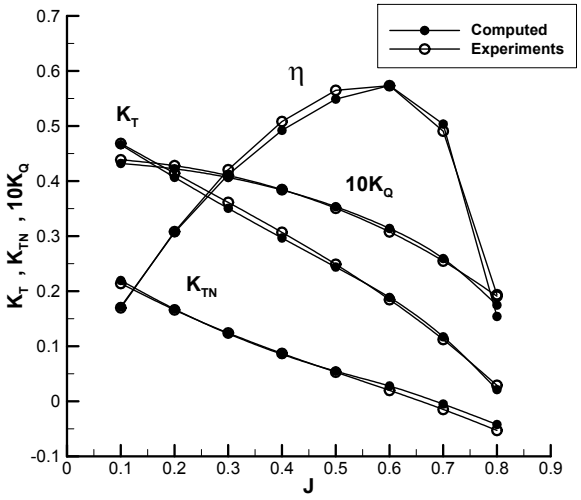

Fig. 3 Comparison between the numerical and experimental results.

In Fig. 3, K_T K_Q K_{TN} and η are the thrust coefficient the torque coefficient the duct thrust coefficient and the efficiency.

RESULTS AND DISCUSSION

To investigate the effect of tip clearance on ducted propeller performance, several models (Ka4-70 in 19A duct) with different tip clearance had been selected. In this paper, tip clearance was changed by expanding the diameter of the duct for maintaining the propeller blades. As the flow field around the propeller shows different character, three levels of advance ratio were chosen to show the tip clearance effect. This ducted propeller reaches the maximum efficiency at about J = 0.6. Therefore, we choose $J = 0.3$ as the low advance ratio, $J = 0.6$ as the middle advance ratio and $J = 0.8$ as the high advance ratio. Some of the computed results will been presented and discussed follow.

Effects on performance of ducted propeller

The flow leaking through the tip clearance causes the change of efficiency. The change of the efficiency with tip clearance size was observed roughly linearly at low advance ration. The level of tip clearance effect is evaluated by the leakage loss slope. Fig. 4 shows the efficiency varies with tip clearance size at different advance ratio. In general, efficiency decreases while the clearance expands. The changing trends is approximately linearly at $J = 0.3$ and $J = 0.6$. Fig. 4(c) shows that efficiency decreases firstly then increases at $J = 0.8$. This implies that the leakage loss is not always roughly linearly at all working condition. It is influenced by the advance ratio. In other words, the leakage loss is related to the ratio of two components (rational velocity and advancing velocity) of the absolute velocity near the clearance.

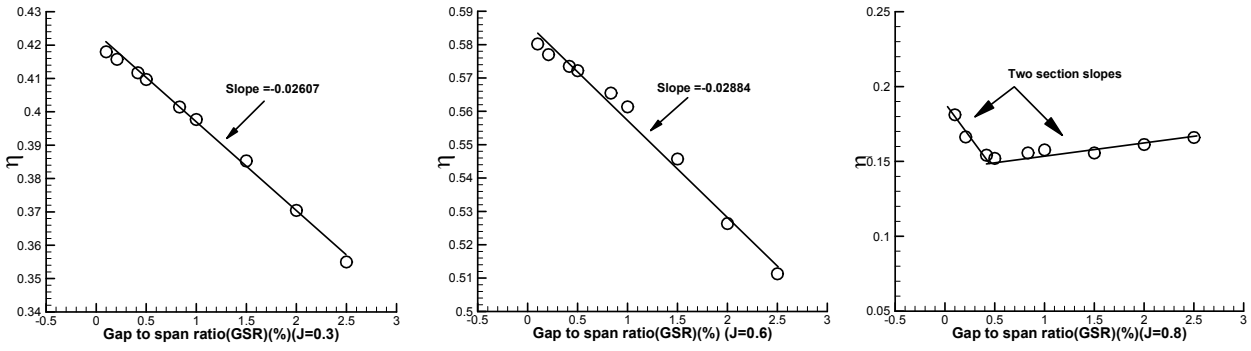

(a) (b) (c)

Fig. 4 Variation of efficiency with tip clearance size at different advance ratio.

For detailed investigation, thrust coefficients and torque coefficients at $J = 0.8$ are given in Fig. 5. We found that thrust and torque coefficients decrease as the gap expands from 0.1 to 0.5 GSR and then increase as the gap expands. The duct thrust curve in Fig. 5(c) can be treated as two lines with slopes as -6.228×10^{-3} and -5.965×10^{-4} respectively. All the three coefficient curves reach the turning point at a GSR near 0.5.

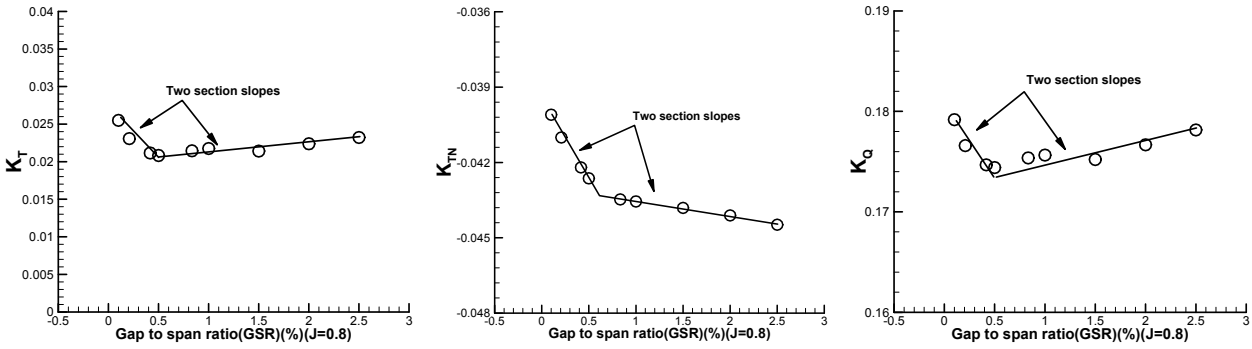

(a) (b) (c)

Fig. 5 Variation of (a) thrust coefficient (b) duct thrust coefficient
(c) torque coefficient with tip clearance size at $J = 0.8$.

Effects on duct and blade loading

Fig. 6 shows the pressure coefficient distribution on the inner duct of ducted propellers with different GSR. The pressure coefficient is defined as:

$$C_p = \frac{p - p_\infty}{0.5\rho U_\infty^2} \tag{5}$$

The distribution of pressure coefficient is strongly influenced by the gap size. Low C_P area expands when GSR decreases. Area 2 is mainly influenced by vortex between two blades at the suction side. Tip vortex causes the decrease of pressure at area 1. Area 3 is near the leading edge tip of the blade .Because the local attack angle at the blade tip is negative at this working condition, pressure at area 3 reverses. Tip vortex breaks down after area 4. It is obvious that pressure on the inner duct is influenced less by the expanding of the gap. Combining with Fig. 5(b) we can conclude that slope of the fore curve is mainly caused by the tip vortex effect on area 1 and 4, the slope after is mainly influenced by flow separation at area 3 and vortex between blades at area 2.

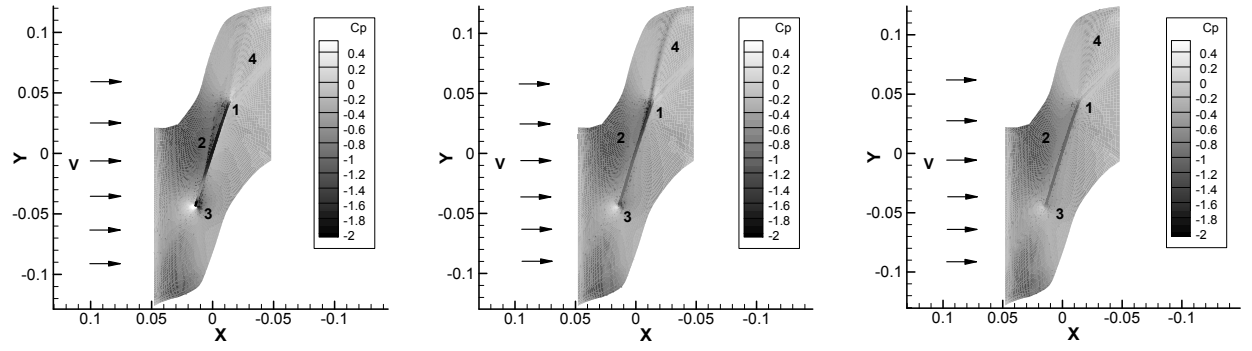

(a) (b) (c)

Fig. 6 Pressure coefficient distribution on inner duct with different gap size (J = 0.8):
(a) GSR = 0.1 (b) GSR = 0.5 (c) GSR = 1.

Fig. 7 shows the pressure coefficient distribution on blade suction side. The distribution of the pressure is almost the same except for the little difference at the blade tip near the leading edge. It is obvious that the influence of gap size mainly concentrate on the blade tip.

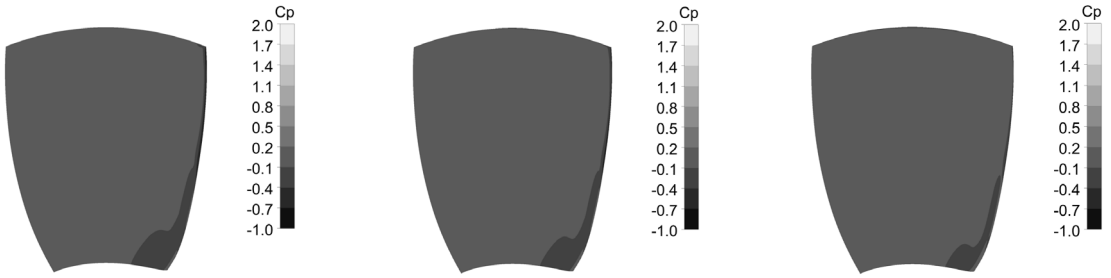

(a) (b) (c)

Fig. 7 Pressure coefficient distribution on the blade with different gap size
(a) GSR = 0.1 (b) GSR = 0.5 (c) GSR = 1.

Fig. 8 shows the blade tip loading at a constant span of 0.98 of different gap. Blade tip loading of GSR below 0.5 is illustrated in Fig. 8(a). In Fig. 8(a), it is obvious that blade tip loading is strongly influenced by the gap size. As the GSR increases from 0.1 to 0.5, the reverse point transfers from 0.19 to 0.27 streamwise. Because of the existing of reversed pressure area at leading edge, the tip vortex origination is pushing back to the trailing edge. When GSR is below 0.5, blade tip loading near the leading edge decreases while loading near the trailing edge increases with the expanding of the gap size. Blade tip loading of GSR above 0.5 is illustrated in Fig. 8(b). It demonstrates that blade tip loading has no relation with the gap size. The reversed points locate at about 0.1 streamwise. Pressure coefficient reaches the maximum at about 0.9 streamwise.

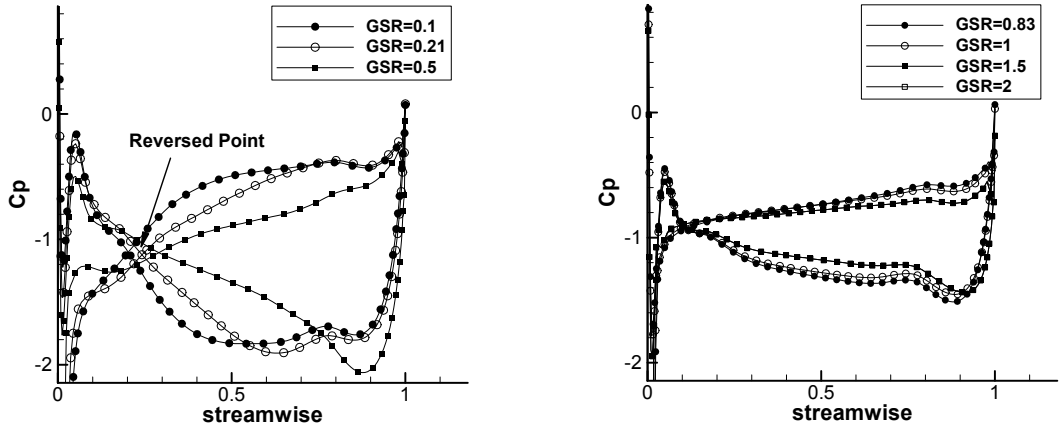

(a) (b)

Fig. 8 Blade tip loading of different GSR at constant span of 0.98 (J = 0.8).

Tip vortex structure

Quatitive studies of flow in turbine, compressor and pump have been done to understand the mechanisms of tip leakage loss. You et al. (2007) found that the tip vortex structure is formed by three parts: the tip-separation vortex, the tip-leakage vortex and the induced vortex. The tip-leakage vortex is caused by the pressure different between the pressure and the suction side. The tip-separation vortex is formed due to flow separation underneath the blade tip. The induced vortex is generated by the tip-leakage vortex. Fig. 9 shows the vortex core in steady state using the λ_2 vortex-identification (Jeong and Hussain, 1995). Compared with Fig. 9(a), tip vortex in Fig. 8(b) has a different structure. Tip leak-age vortex is separated into two parts by the reversed pressures point as show in Fig. 8. In the case $J = 0.8$, tip-leakage vortex near the leading edge originates from the suction side at about 3% to 10% of the chord, and extends toward the pressure side.

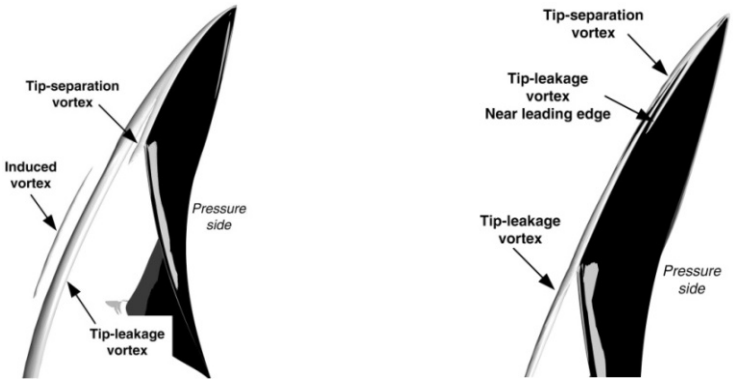

(a) J = 0.6. (b) J = 0.8.

Fig. 9 Illustration of tip vortex core in steady state GSR = 1.

The tip vortex structure is affected not only by the blade loading but also the gap size. Fig. 10 shows vortex line on Y-Z plane (X = 0) in the tip clearance of different GSR. In the case GSR=0.1, as shown in Fig. 10(a), a main large vortex is formed at the beginning of the clearance near the inner duct. Several shedding vortex is found after the main vortex. These vortices are formed because of the injection of the fluid through the clearance into the boundary layer on the inner duct. Fig. 10(c) shows planar vortex line of GSR = 0.5 and 1 respectively. In the case GSR=1, the main vortex is near the blade tip face. This vortex is formed mainly due to the flow separation at the tip. The interaction of the main flow through the clearance with the boundary layer of the blade also contributes to the vortex near the blade tip face.

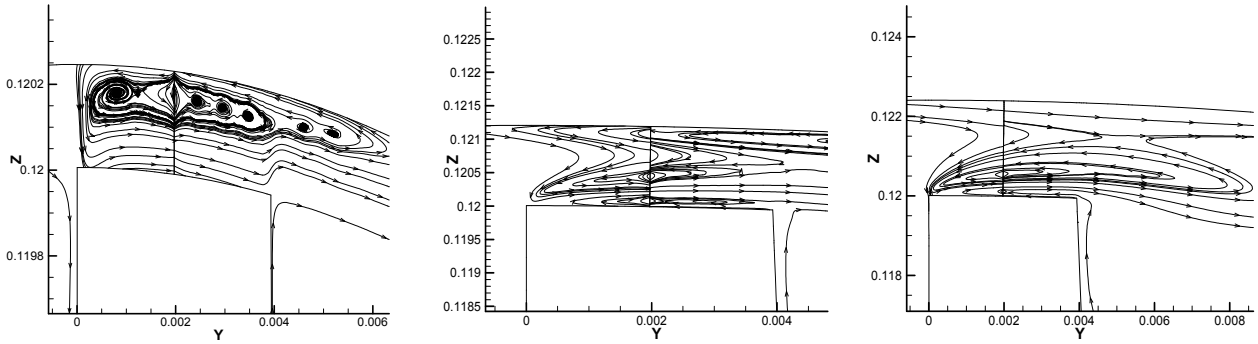

(a) GSR = 0.1. (b) GSR = 0.5. (c) GSR = 1.

Fig. 10 Illustration of vortex line on the Y-Z (X=0) plane at the tip clearance (J = 0.8).

As the advance ratio increases to 0.8, the attack angle at the blade tip reduces to negative. Inversed pressure appears near the leading edge at the blade tip. A different vortex structure was generated by this inversed pressure area shown in Fig. 9(b). This vortex structure can be separated to two parts by the reversed point. As the pressure downstream rose, the vortex break-down causing the loss of energy. The first energy loss was before the reversed point as shown in Fig. 9(b). The second energy loss begins from the revered point to downstream. As shown in Fig. 10(a), the clearance was occupied by the tip separation vortex when the clearance was small enough. The shedding vortex breakdown appeared in the clearance at high advance ratio at small GSR. When the GSR was up to 1, the vortex breakdown was not that much in the clearance as the GSR 0.1. This can be the explanation of the broken line in Figs. 4 and 5.

Effects on turbulence kinetic energy

Fig. 11 shows the Mass Circle Average (MCA) turbulence kinetic energy on the inlet to outlet line which is defined as

$$\bar{k} = \frac{1}{\dot{m}} \int_A k \rho \vec{V} \bullet \hat{n} dA \tag{6}$$

where

$$\dot{m} = \int_A \rho \bar{V} \bullet \hat{n} dA \tag{7}$$

The blade boundary layer separation and the clearance leakage flow generate strong turbulence kinetic energy. The clearance shows no effect on the turbulence kinetic energy from the inlet to about 50% streamwise. The turbulence kinetic energy increases with the expanding of the clearance after 50% streamwise. It is obvious that the flow through the larger clearance generates more turbulence kinetic energy. The influence of the clearance on turbulence kinetic energy mainly locates after 50% streamwise.

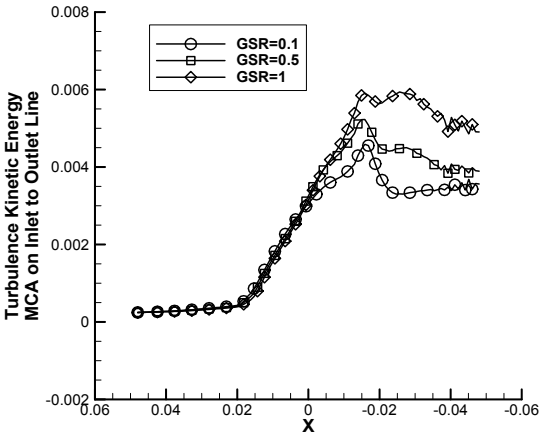

Fig. 11 Mass circle average (MCA) turbulence kinetic energy from the inlet to outlet.

CONCLUSIONS

A ducted propeller with different size of tip clearance has been presented to investigate the influence of the tip clearance to ducted propeller. This analysis was carried out with RANS method. Several validation studies have been done to detect the influence of the gird and the turbulence model on simulations. The influences of the clearance on ducted propeller are reflected in five aspects mainly.

1) The thrust and torque coefficient decrease linearly with the clearance expanding at low advance ratio. While at high advance ratio, these coefficients decrease with the clearance expanding to a GSR of 0.5 then increase with its expanding. At high advance ratio, the main cause of the nonlinear of loss slope is the reversed pressure at leading edge.
2) The clearance size has little effect on the pressure distribution on the blade below 0.98 spanwise.
3) Pressure distribution on the inner duct and blade tip was influence strongly by the tip clearance below a GSR of 0.5. The mainly influence area locates at the suction side and near the leading edge.
4) The vortex structure in the clearance changes from a shedding vortex to one big separation vortex with the expanding of the clearance. This vortex structure and the blade tip loading affect each other before the trailing edge.
5) The bigger clearance generates more turbulence kinetic energy. The influence on the turbulence kinetic energy mainly located after 50% streamwise.

The negative attack angle at high advance ratio caused the inversed pressure area near the leading edge. The vortex structure was influenced strongly by the inversed pressure area. The shedding vortex breakdown loss more energy can be considered as the explanation of two section slope at high advance ratio.

ACKNOWLEDGEMENT

This research was supported by the Fundamental Research Funds for the Central Universities (Grant NO.3102014JCQ 01007).

REFERENCES

Abdel-maksound, M. and Heinke, H., 2002. Scale effects on ducted propellers. *Proceedings of the 24th Symposium on Naval Hydrodynamics*, Fukuoka, Japan, July 2002, pp.744-759.

Ansys, 2012. *Solver theory guide, Release 14.5*. Canonsburg: Ansys Inc.

Berchiche, N. and Janson, C.E., 2008. Grid influence on the propeller open-water performance and flow field. *Ship Technology Research*, 55, pp.87-96.

Booth, T., 1985. *Importance of tip clearance flows in turbine design, VKI lecture series, 1985-05: tip clearance effects in axial turbomachines*. Belgium: Von Karman Institute for Fluid Dynamics.

Chima, R.V., 1998. Calculation of tip clearance effects in a transonic compressor rotor. *Journal of turbomachinery*, 120(1), pp.131-140.

Hoekstra, M., 2006. A RANS-based analysis tool for ducted propeller systems in open water condition. *International shipbuilding progress*, 53(3), pp.205-227.

Hsiao, C.T. and Pauley, L.L., 1999. Numerical computation of tip vortex flow generated by a marine propeller. *Journal of Fluids Engineering*, 121(3), pp.638-645.

Hughes, M., Kinnas, S. and Kerwin, J., 1992. Experimental validation of a ducted propeller analysis method. *Journal of fluids engineering*, 114(2), pp.214-219.

Jeong, J. and Hussain, F., 1995. On the identification of a vortex. *Journal of fluid mechanics*, 285, pp.69-94.

Kerwin, J.E., Kinnas, S.A., Lee, J.T. and Shin, W.Z., 1987. *A surface panel method for the hydrodynamic analysis of ducted propellers*. Massachusetts: DTIC Document.

Mccarter, A.A., Xiao, X. and Lakshminarayana, B., 2001. Tip clearance effects in a turbine rotor: part II-velocity field and flow physics. *Journal of turbomachinery*, 123(2), pp.305-313.

Moon, I.S., Kim, K.S. and Lee, C.S., 2002. Blade tip gap flow model for performance analysis of waterjet propulsors. *Proceedings of International Association for Boundary Element Methods.* University of Texas, Austin, 28-30 May 2002.

Morgut, M. and Nobile, E., 2012. Influence of grid type and turbulence model on the numerical prediction of the flow around marine propellers working in uniform inflow. *Ocean Engineering*, 42, pp.26-34.

Oosterveld, M.W.C., 1970. *Wake adapted ducted propellers*. TU Delft: Delft University of Technology.

Park, W.G., Jung, Y.R. and Kim, C.K., 2005. Numerical flow analysis of single-stage ducted marine propulsor. *Ocean engineering*, 32(10), pp.1260-1277.

Peng, H.H., Qiu, W. and Ni, S., 2013. Effect of turbulence models on RANS computation of propeller vortex flow. *Ocean Engineering*, 72(1), pp.304-317.

Xiao, X., Mccarter, A.A. and Lakshminarayana, B., 2001. Tip clearance effects in a turbine rotor: Part I-pressure field and loss. *Transactions of the ASME-T-Journal of Turbomachinery*, 123(2), pp.296-304.

Yaras, M. and Sjolander, S., 1992. Effects of simulated rotation on tip leakage in a planar cascade of turbine blades: part I-tip gap flow. *Journal of turbomachinery*, 114(3), pp.652-659.

Yaras, M., Sjolander, S. and Kind, R., 1992. Effects of simulated rotation on tip leakage in a planar cascade of turbine blades: part II-downstream flow field and blade loading. *Journal of turbomachinery*, 114(3), pp.660-667.

You, D., Mittal, R., Wang, M. and Moin, P., 2002. Large-eddy simulation of a rotor tip-clearance flow. *40th AIAA Aerospace Sciences Meeting & Exhibit*. American Institute of Aeronautics and Astronautics, Reno, Nevada, 14-17 January 2002.

You, D., Mittal, R., Wang, M. and Moin, P., 2004. Computational methodology for large-eddy simulation of tip-clearance flows. *AIAA journal*, 42(2), pp.271-279.

You, D., Wang, M., Mittal, R. and Moin, P., 2003. Study of rotor tip-clearance flow using large-eddy simulation. *41st Aerospace Sciences Meeting and Exhibit.* American Institute of Aeronautics and Astronautics, Reno, Nevada, 6-9 January 2003.

You, D., Wang, M., Moin, P. and Mittal, R., 2006. Effects of tip-gap size on the tip-leakage flow in a turbomachinery cascade. *Physics of Fluids (1994-present)*, 18, pp.105102.

You, D., Wang, M., Moin, P. and Mittal, R., 2007. Large-eddy simulation analysis of mechanisms for viscous losses in a turbomachinery tip-clearance flow. *Journal of Fluid Mechanics*, 586, pp.177-204.